TABLE I
DESIGN PARAMETERS FOR LOG-PERIODIC MONOPOLE ARRAY

Array Parameters	
τ	0.94
σ	0.08
S	10.6°
Number of elements	18
Height of element #1	0.125 m
Structure bandwidth	2.86:1
Boomlength	0.438 m
h/a	122.5
Feeder Parameters	
$r = d_2/d_1$	8.0
Impedance modulation ratio	71.3:50
Dielectric constant	2.65
Dielectric thickness	0.159 cm ($\frac{1}{16}$ in)
Microstrip width ratio	0.242:0.459 (cm/cm)
Discontinuity capacitance	0.0098 pF
Truncation length	0.245 m
λ_r	0.680

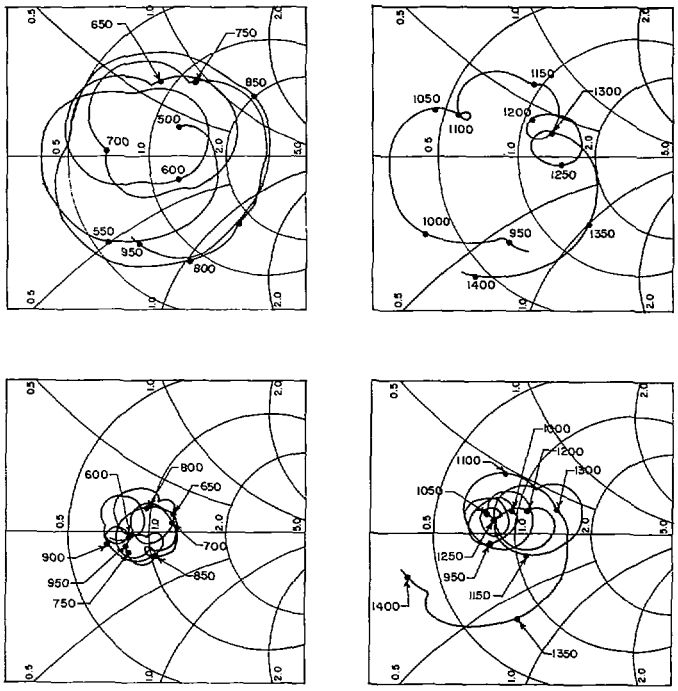

Fig. 4. Swept frequency measurements of input impedance of LP monopole of Table I—upper plots, unmodulated feeder; lower plots, modulated feeder. (Frequencies in MHz).

value is less than 1.9. Although it has been demonstrated that an LP monopole array can be directly matched to 50 Ω within its feed network, this particular impedance level is not necessarily optimum insofar as frequency independent performance is concerned.

REFERENCES

[1] R. L. Carrel, "Analysis and design of the log-periodic dipole antenna," Antenna Lab., Univ. Illinois, Urbana, Tech. Rep. 52, Contract AF33(616)-6079, 1961.
[2] P. G. Ingerson and P. E. Mayes, "Log-periodic antennas with modulated impedance feeders," *IEEE Trans. Antennas Propagat.*, vol. AP-16, pp. 633–642, Nov. 1968.
[3] D. E. Isbell, "Log-periodic dipole arrays," Antenna Lab., Univ. Illinois, Urbana, Tech. Rep. 39, Contract AF33(616)-6079, 1959.
[4] P. B. Green and P. E. Mayes, "A log-periodic monopole array with a modulated impedance microstrip feeder," Antenna Lab., Univ. Illinois, Urbana, Rep. 73-2, Jan. 1973.
[5] E. C. Jordan and K. G. Balmain, *Electromagnetic Waves and Radiating Systems*. Englewood Cliffs, N. J.: Prentice-Hall, 1968.

VLF Antarctic Antenna: Impedance and Efficiency

R. RAGHURAM, R. L. SMITH, AND TIMOTHY F. BELL

***Abstract*—A 21-km horizontal very-low frequency (VLF) antenna has been constructed at Siple Station, Antarctica. This antenna is to be used to inject VLF waves into the magnetosphere in order to perform wave particle interaction experiments. In the present paper, the properties of this antenna are analyzed and its impedance and efficiency calculated. The electrical properties of the ice layer beneath the antenna are modeled. The ice is represented by several layers, each with a different dielectric constant and conductivity. A variational method due to Galejs [2] for an antenna in a stratified dielectric is used. In this method the cylindrical antenna is replaced by an equivalent strip antenna so that the entire geometry is planar. The efficiency is calculated as a function of frequency for different lengths of the antenna. It is found that the antenna is most efficient near its antiresonant frequency. The optimum length for efficient operation at a given frequency is discussed. It is shown that the antenna has an efficiency greater than 2 percent over more than a 2 to 1 frequency range. Some advantages of the Siple antenna, as compared with other horizontal and vertical antennas, are pointed out.**

I. INTRODUCTION

The very low frequency (VLF) antenna analyzed in this report is located at Siple Station, Antarctica (76°S, 84°W). The antenna is a horizontal dipole, 21.4 km long and supported on poles approximately 12 ft above an ice layer of approximately 2-km thickness. The spacing between the supporting poles is 200 ft and the maximum sag between poles is approximately 2 ft. The antenna is to be used for transmitting and receiving VLF signals for studies of the magnetosphere. In particular it will be used as a device to inject VLF waves into the magnetosphere in order to perform wave-particle interaction experiments. Experiments of primary interest are those connected with the production of VLF emissions, enhanced energetic particle precipitation, micropulsation, aurora, and ionospheric density perturbations. In this report the characteristics of the antenna as a transmitting device are analyzed in the frequency range 1–18 kHz. The ice layer, approximately 2 km thick, considerably improves the radiation efficiency. Its presence, however, complicates the analysis.

Guy [1] studied the characteristics of long antennas buried in ice. He assumed the ice to be homogeneous and semi-infinite. In reality, the dielectric constant of ice varies greatly with depth and at Siple Station the ice is not thick enough to allow us to neglect the ground beneath it. Consequently, a better model is one in which the ice is represented by several layers of finite thickness, and the effect of the ground is taken into account. The approach of Galejs [2] for an antenna imbedded in several dielectric layers seems to be well suited to this problem. The use of the variational principle in his approach obviates the necessity of accurately knowing the wavenumber. Galejs' method, with a few minor changes, is used in the analysis.

Section II gives the formulation of the problem. Section III describes how the expressions for impedance and efficiency are derived. Section IV describes the ice properties. Section V contains a discussion of the results. The conclusions are stated in Section VI.

II. FORMULATION OF PROBLEM

In the approach used by Galejs [2], the entire geometry, including the antenna, is planar. The cylindrical antenna is replaced by an equivalent strip antenna. According to Kraus [3], the equivalent

Manuscript received July 10, 1973; revised September 26, 1973. This work was supported in part by the Office of Polar Programs of the National Science Foundation under Grant GV-28840X, in part by the Office of Naval Research under Contract N00014-67-A-0112-0012, and in part by the Air Force Office of Scientific Research under Contract F-4462-72-C-0058.
The authors are with the Radioscience Laboratory, Stanford University, Stanford, Calif. 94305.

width for the strip antenna is twice the diameter of the cylindrical antenna. This replacement is valid as long as the nearest dielectric layer is at least a few wire diameters away.

Fig. 1 shows the geometry of the antenna and the associated layers. The antenna lies in the xy plane at $z = 0$. The thickness of the antenna is assumed to be negligible in the z direction. The strip is 2ϵ wide in the y direction and $2l$ long in the x direction. We assume that $\epsilon \ll l$. The separation of the two halves of the antenna is considered to be very small so that the electric field produced by the voltage generator is a delta function of value $-V_0\delta(x)\Pi(y/\epsilon)$, where V_0 is the impressed voltage, $\delta(x)$ the well known Dirac delta function and $\Pi(y/\epsilon)$ is the box-car function

$$\Pi(y/\epsilon) = \begin{cases} 1, & \text{for } |y/\epsilon| < 1 \\ 0, & \text{for } |y/\epsilon| > 1. \end{cases}$$

For $|x| > 0$, the electric field at the antenna is related to the internal impedance of the antenna. Let Z^i = internal impedance per unit length (Ω/m) and z^i = internal surface impedance (Ωm/m). Since the width is 2ϵ,

$$Z^i = z^i/2\epsilon$$

and the current in the antenna is

$$I(x) = 2\epsilon J_s(x,y)$$

where J_s the surface current density (A/m), is assumed independent of y for $|y| < \epsilon$. Denote the input current by $I(0)$ and the input impedance by Z, so that $V_0 = Z \cdot I(0)$. The tangential electric field on the antenna and in the gap can be written

$$E^t\Pi(x/l)\Pi(y/\epsilon) = z^i J_s(x,y) - V_0\delta(x)\Pi(y/\epsilon). \tag{1}$$

Multiplying (1) by J_s and integrating over the surface we get

$$Z = \frac{Z^i}{I^2(0)}\int_{-l}^{l} I^2(x)\,dx - \frac{1}{I^2(0)}\int_{-l}^{l}\int_{-\epsilon}^{\epsilon} (\boldsymbol{E}\cdot\boldsymbol{J}_s)\,dx\,dy. \tag{2}$$

The advantage of the preceding formulation is that the value of the terminal impedance is stationary with respect to small changes in the current from the true current. This formulation of the antenna impedance was first introduced by Storer [4] and was also discussed by King [5]. The specific application to the flat plate antenna was described by Galejs [2]. Galejs did not include the internal impedance term, but this is relatively easy to add.

In theory, one would find the impedance by setting the variation of Z with respect to all relevant parameters equal to zero. The current distribution is then found, reinserted into the original equation, and the impedance found. That procedure is extremely difficult. In practice one assumes a "trial function" with only a few parameters. These parameters are varied until a stationary solution is found. The trial function suggested by Galejs is

$$J_s(x,y) = \{\sin k_a(l - |x|) + Q[1 - \cos k_a(l - |x|)]\}f(y)$$

where Q is a complex parameter, k_a the antenna propagation constant, l the antenna half-length, and

$$f(y) = 1/2\epsilon\Pi(y/\epsilon)$$

where ϵ is the antenna half-width. The expression on the right may be multiplied by an arbitrary constant, but this constant is in essence immaterial. Although Galejs considered k_a to be real, there are a number of advantages in considering k_a to be complex. If l is a multiple of $2\pi/k_a$ and k_a is real, then the trial function above vanishes for $x = 0$, and the computation becomes indeterminant. If the antenna were considered as a lossy transmission line one would get a complex value for its propagation constant. This suggests that a complex value for k_a will yield a current distribution more nearly representative of the true current.

III. Derivation of Impedance and Efficiency Expressions

The electromagnetic field can be expressed as a sum of two Hertzian potentials in a particularly simple way for the planar geometry assumed here. The two potentials are the transverse electric and the transverse magnetic potentials. The electric and magnetic fields can be obtained from the Hertzian potentials in the usual way [2].

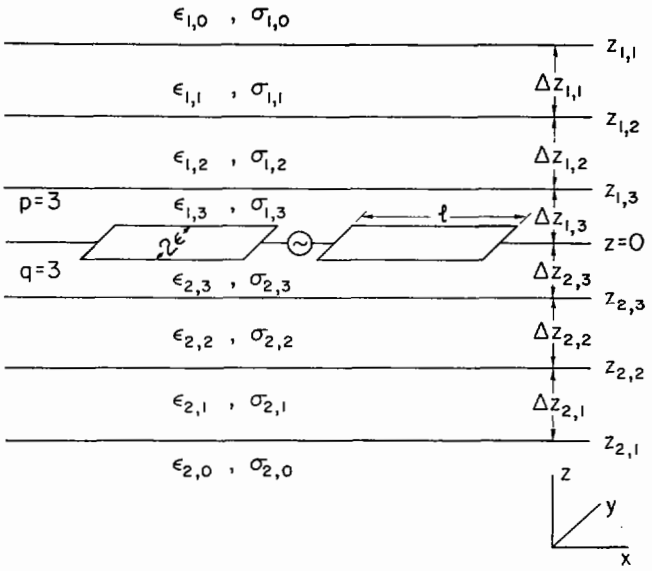

Fig. 1. Antenna and layer geometry.

The potentials for each stratified layer may be found by satisfying the boundary condition at each interface. The expression for the input impedance can then be written as

$$Z = \frac{\gamma_{AA}'\gamma_{BB}' - \gamma_{AB}'^2}{F_B^2\gamma_{AA}' - 2F_AF_B\gamma_{AB}' + F_A^2\gamma_{BB}'} \tag{3}$$

where

$$\gamma_{AA}' = \gamma_{AA} + \frac{Z^i}{2k_a}[2k_al - \sin 2k_al]$$

$$\gamma_{AB}' = \gamma_{AB} + \frac{Z^i}{2k_a}[3 + \cos 2k_al - 4\cos k_al] \tag{4}$$

$$\gamma_{BB}' = \gamma_{BB} + \frac{Z^i}{2k_a}[6k_al + \sin 2k_al - 8\sin k_al]$$

and the quantities γ_{AA}, γ_{AB}, γ_{BB}, F_A, and F_B appearing in (3) and (4) are defined as in [2, eq. (8)-(14)].

Equation (3) is similar in form to [2, eq. (8)], but differs from this expression in content since we have included the internal impedance as calculated from the first term on the right-hand side of (2). The internal impedance should be included in the total impedance when the stationary character of the impedance is used to determine the current distribution parameter Q.

The power radiated to the outermost regions can be evaluated from [2, eq. (17)] and the radiation resistance R_r from [2, eq. 23].

The efficiency κ can then be written as

$$\kappa = \frac{R_r}{R.P.[Z]}. \tag{5}$$

IV. Model Chosen for Ice in Antarctica

A. Dielectric Constant of Pure Ice

The dielectric constant (complex) of pure ice is assumed to be given by the Debye model

$$\epsilon = \epsilon' - j\epsilon'' = \epsilon_\infty + \frac{\epsilon_0 - \epsilon_\infty}{1 + (f/f_c)^2}\left(1 - j\frac{f}{f_c}\right)$$

where ϵ_0 is the dielectric constant at dc, ϵ_∞ is the limiting HF dielectric constant, and f_c is a function of temperature.

The temperature dependence of f_c is given by

$$f_c = A\exp(-B/RT)$$

where T is the absolute temperature, R is the universal gas constant,

and A and B are constants determined experimentally by Auty and Cole [6].

B. Dielectric Constant as a Function of Relative Density

The surface layers of the ice in Antarctica contain a mixture of air and ice. Assuming the ice to exist in the form of spherical particles, the theory in Polder and Van Santen [7] can be used to find the dielectric constant as a function of density. Assuming the density of air to be negligible compared to that of ice, one can write

$$V_i = \frac{\rho}{\rho_i}$$

$$\epsilon_r = \epsilon_{r_i} V_i f(\epsilon_r) \tag{6}$$

where

$$f(\epsilon_r) = \frac{1}{1 + \frac{1}{3}(\epsilon_{r_i}/\epsilon_r - 1)}.$$

V_i is the relative volume of ice, ρ is the density of the mixture, ρ_i is the density of pure ice, ϵ_r is the real part of the dielectric constant of the mixture, and ϵ_{r_i} is the real part of the dielectric constant of pure ice. The imaginary part of the dielectric constant ϵ_i is similarly evaluated as

$$\epsilon_i = \epsilon_{ii} V_i f(\epsilon_r)$$

where ϵ_{ii} is the imaginary part of the dielectric constant of pure ice.

C. Temperature and Density Variation of Antarctic Ice

Four regions are chosen to describe the density variation of the ice with depth [8]: 1) within 0–10 m the relative density increases linearly from 0.45 to 0.65, 2) at depths of 10–130 the relative density increases linearly from 0.65 to 0.85, while 3) between 130–1000 the relative density increases linearly from 0.85 to 0.917, the relative density of pure ice, and 4) at 1000 m and below the relative density is approximately constant at 0.917.

Data on the temperature variation with depth is rather scarce; however, the results from drilling down to the bedrock at Byrd Station by Gow *et al.* [9] can be used as a guideline. The mean annual temperature at Siple Station is almost the same as that at Byrd Station [10]. Temperature variations occurred only in the surface layer. The temperature was constant throughout the year below a depth of about 20 m. The temperature from about 20–1000m was roughly constant at −28°C. Below 1000 m the temperature rose fairly linearly to −1.6°C at 2164 m. Water was present in a layer at least a millimeter deep between the bedrock and the ice.

D. Final Model Chosen

On the basis of the results stated above, a five-layered model was chosen for the ice, as shown in Table I. The temperature of the uppermost layer depends on the surface temperature and hence varies from day to day. The temperature given is the value used in the calculations.

The total depth of 1900 m was chosen as an approximate mean for the area around Siple. Sufficient data are not available to make a better estimate.

The nature of the rock below the ice is also not well known. It was assumed to be wet rock with $\epsilon_r = 10$ and conductivity $\sigma = 10^{-3}$ mho/m.

To take impurities into account, a conductivity of 3.34×10^{-6} mho/m was added to the ice at all temperatures and frequencies. This value is comparable to impurity conductivities measured by Watt and Maxwell [11] in glaciers and gives a good fit between the calculated and measured input impedance values of the antenna. The ice model used gives values of the dielectric constant comparable to bulk values estimated by Peden *et al.* [12] and Webber and Peden [13]. For example, at 12.8 kHz in these two papers the dielectric constant was estimated to be $6\text{-}j14$. The values obtained from our model vary from $14.60\text{-}j34.74$ for the bottom layer to $3.05\text{-}j7.16$ for the layer extending from 10–1000m.

TABLE I

Depth of Layer (m)	Temperature (°C)	Density
0–10	−10	0.55
10–1000	−28	0.87
1000–1300	−24	0.917
1300–1600	−14	0.917
1600–1900	−4	0.917

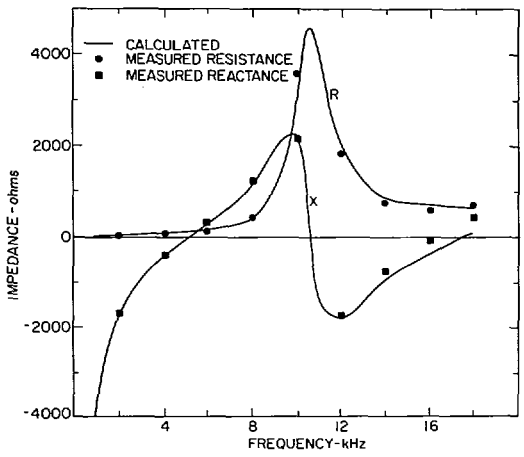

Fig. 2. Input impedance of antenna as function of frequency.

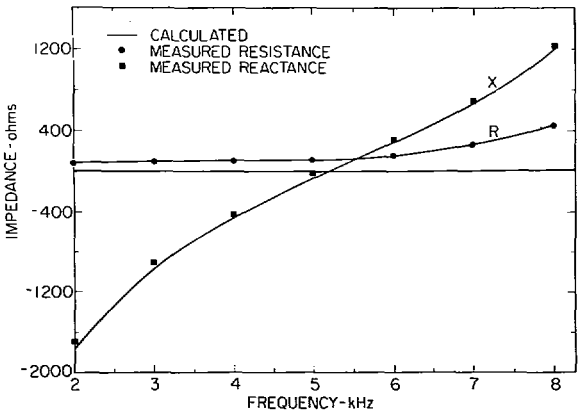

Fig. 3. Region between 2 and 8 kHz in Fig. 2 shown on expanded scale.

V. Discussion of Results

A. Impedance

The input impedance of the antenna was calculated using (3). The computations were done on a digital computer. Figs. 2 and 3 show that a comparison between the measured and calculated values is good for frequencies up to 14 kHz. For frequencies below 3 kHz the calculated values of the input resistance are higher than the measured values. This is not seen in the figures because of the scale used. These deviations are probably due to: 1) the dielectric constant and thickness of the ice layer not being known accurately, 2) the sag in the antenna wire which changes the length of the antenna, and 3) the effect of the ionosphere which is particularly important at low frequencies.

B. Efficiency

The efficiency was calculated using (5) and is plotted as a function of frequency in Fig. 4. Three antenna lengths are considered, the measured length of 21.4 km as well as the lengths of 28.1 and 53.4 km. The respective half-wave resonance frequencies for these lengths are calculated to be 5.4, 4.0, and 2.4 kHz. The measured resonant frequency of the 21.4 km antenna was 5.1 kHz; thus agreement between theory and measurement is reasonable.

From the curves plotted for $2l = 28.1$ km and $2l = 53.4$ km, it can be seen that the same general shape is predicted for the efficiency curve when the length of the antenna is changed.

In general, the point of maximum efficiency occurs near the antiresonant frequency, i.e., the frequency at which $2lk_a \cong 2\pi$. The peak

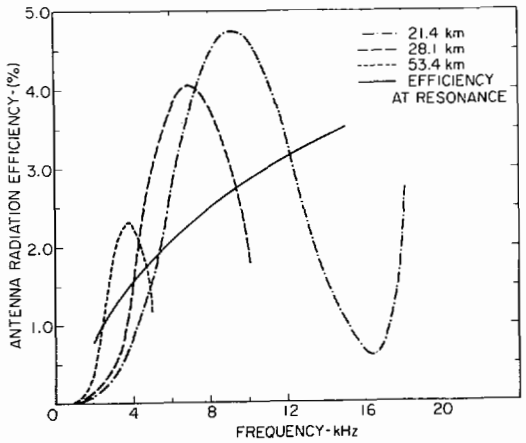

Fig. 4. Efficiency as function of frequency for different antenna lengths.

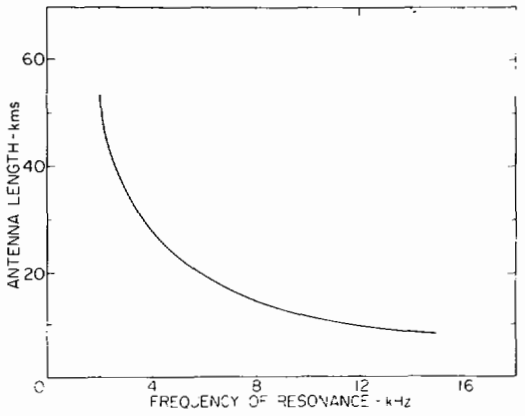

Fig. 5. Resonant antenna length required as function of frequency. For antenna in free space, curve would be rectangular hyperbola.

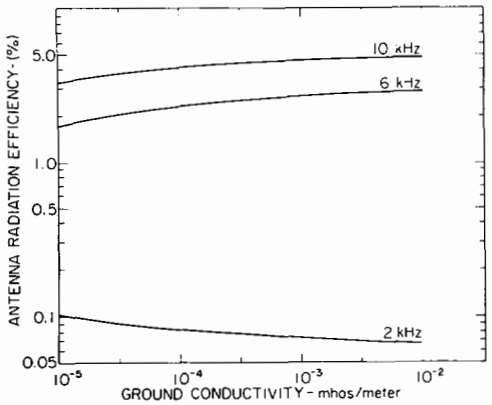

Fig. 6. Efficiency as function of ground conductivity for different frequencies.

efficiency decreases with increasing antenna length because: 1) the peak efficiency occurs at a lower frequency where losses are greater in the ice, and 2) the internal impedance increases with increasing length. For example, with $2l = 53.4$ km the resistive part of the internal impedance is 31.2 Ω out of a total resistance of 75.8 Ω near the resonant frequency. With $2l = 21.44$ km it is only 19.6 Ω out of a total resistance of 116.7 Ω near resonance.

Also shown in Fig. 4 is a curve giving the efficiency at resonance of a half-wave antenna of unspecified length. For this curve the antenna length is a floating parameter whose value at any frequency can be obtained from Fig. 5. The efficiency is higher at higher resonant frequencies, as might be expected.

Fig. 5 shows the antenna length required for different resonant frequencies. The curve is approximately a rectangular hyperbola, which means that the wavenumber along the antenna is approximately a linear function of the frequency.

Fig. 6 shows the effect of varying the conductivity of the ground, upon which the ice slab rests, on the antenna efficiency. It is seen that as long as the conductivity is greater than 10^{-3} mho/m, the efficiency is roughly independent of the conductivity. Weber and Peden [13], in their calculation of the dielectric constant of the Antarctic ice, also found that their method was relatively insensitive to the conductivity of the layer beneath the ice, as long as it was greater than 10^{-3} mho/m. The ground conductivity in most parts of the world is greater than this value. The conductivity of water, especially that of sea water, is also at least equal to this value. So whatever the nature of the layer beneath the ice, it is most probable that it has a conductivity greater than 10^{-3} mho/m. The use of this value for the ground conductivity, in the curves plotted in Figs. 2–4, is hence reasonable. The relative dielectric constant (real) of the ground was assumed to be 10 for the efficiencies plotted in Fig. 6. The efficiencies were calculated for an antenna length of 21.4 km. The efficiencies plotted for this antenna length in Fig. 4 hence correspond to those plotted in Fig. 6 for a conductivity of 10^{-3} mho/m.

To study the effect of the thickness of the ice layer on the efficiency, a single layered model was used for the ice. The frequency chosen was 6 kHz. A bulk relative dielectric constant of $14.87 - j28.65$ was used [12]. The calculated efficiency dropped from 2.39 percent to 0.10 percent when the thickness was reduced to 100m from 1900m. It dropped further to 0.038 percent when the ice layer was removed and the antenna was over the ground.

C. Frequency Range of Efficient Operation

Fig. 4 shows that, for the present length, the antenna efficiency exceeds 2 percent over the approximate frequency range 5–14 kHz. However, the antenna input impedance varies considerably over this frequency range. Hence the task of matching (conjugate impedance) the antenna impedance to the transmitter output impedance over this large frequency range is made difficult.

Let the system efficiency be defined as the ratio of the radiated power to the maximum transmitter power output. Assuming ideal matching, the overall system efficiency will approach one-half of the antenna efficiency. With the present system at Siple, ideal matching is possible only over the frequency range 4–8 kHz. However, in the near future, a new transmitter will be installed which will allow matching over the range 1–20 kHz. This new system will provide an overall system efficiency which can be as large as 1 percent over the approximate frequency range 5–14 kHz. Since the maximum transmitter power output over this frequency range exceeds 100 kW, the radiated power should exceed 1 kw in the 5–14 kHz band. Experience indicates that this level of radiated power will be ample to perform a wide variety of wave-particle interaction experiments in the magnetosphere. For instance, recent tests with the present transmitter at 4.5 and 5.5 kHz indicate that even at reduced power (50-kW transmitter output) the radiated VLF waves have sufficient amplitude to reach 17 000-km altitude and strongly perturb the energetic particle population in the magnetosphere, producing VLF emissions as well as wave amplification.

VI. Conclusions

From the calculations it is estimated that the Siple antenna has an efficiency greater than 2 percent over the approximate frequency range 5–14 kHz. The maximum efficiency occurs near the antiresonant frequency, approximately 10 kHz, and has the value of approximately 5 percent.

The Siple antenna is superior in many ways to existing VLF antennas. Most present day VLF transmitting systems use vertical antennas. This is mainly because over common types of ground, vertical antennas can be made more efficient than horizontal antennas at VLF frequencies. However, vertical antennas, as Seeley and Wiborg [14] point out, have a number of limitations. They require large and costly high conductivity ground planes. Their lengths are usually much shorter than a wavelength and so they have low radiation resistances and high Q, i.e., their input impedances consist of a large capacitive part and a relatively small resistive part. When the power fed to such an antenna is increased, high voltages appear across the tuning inductance terminals which may result in insulator breakdown [15]. The vertical antenna is thus a voltage limited device, especially in the low frequency end of the VLF band. Vertical antennas also tend to have low bandwidths because of their high Q.

Horizontal antennas do not suffer from the aforementioned limitations. They are relatively inexpensive to construct. They can ideally be made long enough that they are resonant. Furthermore, by terminating a horizontal antenna with its characteristic impedance, one can get very large bandwidths. For a relatively large dip angle such as that at Siple Station, the transmission coefficient at the lower ionospheric boundary for the whistler mode is maximum for angles of incidence close to 0° [16]. The radiation pattern of a horizontal antenna is, therefore, better suited for coupling into the ionosphere. Scarabucci [16] also found that the transmission coefficient was about the same for both horizontal and vertical polarization at low angles of incidence. So on the whole, a horizontal antenna is better for coupling VLF energy into the ionosphere. However, horizontal antennas need a low conductivity ground plane to be efficient. The ice layer at Siple makes an excellent low conductivity ground plane. (Alternatively, the ice can be considered as an insulating layer between the antenna and the conducting ground.) The efficiency of the Siple antenna compares very favorably with most vertical antennas in the low frequency end of the VLF band. For example, the vertical monopole at North Cape, Australia, constructed at a cost of $25 million, has a calculated system efficiency of only 4 percent at 10 kHz [14]. The Siple antenna, constructed at a small fraction of this cost, has a calculated system efficiency greater than 2 percent at 10 kHz. Thus it is possible to obtain all the advantages of horizontal antennas, without sacrificing efficiency or economy, by taking advantage of the natural terrain.

Acknowledgment

The authors wish to thank E. Paschal for making available the impedance measurements on the antenna. The authors are also thankful to J. Katsufrakis, Prof. R. A. Helliwell, and Dr. C. G. Park for their suggestions at various stages of the project.

References

[1] A. W. Guy, "The characteristics of long antennas buried in polar ice," Dep. Elec. Eng., Univ. Wash., Seattle, Tech. Rep. 101, 1966.
[2] J. Galejs, "Driving point impedance of linear antennas in the presence of a stratified dielectric," *IEEE Trans. Antennas Propagat.*, vol. AP-13, pp. 725–736, Sept. 1965.
[3] J. D. Kraus, *Antennas*. New York: McGraw-Hill, 1950.
[4] J. E. Storer, "Variational solution to the problem of the symmetrical cylindrical antenna," Cruft Lab., Harvard Univ., Cambridge, Mass., Tech. Rep. 101, 1951.
[5] R. W. P. King, *Theory of Linear Antennas*. Cambridge, Mass.: Harvard Univ., 1956.
[6] R. P. Auty and R. H. Cole, "Dielectric properties of ice and solid D_2O," *J. Chem. Phys.*, vol. 20, p. 1309, 1952.
[7] D. Polder and J. H. Van Santen, "The effective permeability of mixtures of solids," *Physica*, vol. 12, p. 257, 1946.
[8] V. S. Luchininov and V. N. Rudakov, "Electromagnetic methods for studying the Antarctic snow and ice cover," *Zh. Tekh. Fiz.*, vol. 38, p. 1772, Oct. 1968.
[9] A. J. Gow, H. T. Ueda, and D. E. Garfield, "Antarctic ice sheet: Preliminary results of first core hole to bedrock," *Science*, vol. 161, p. 1011, 1968.
[10] H. Shimuzu, "Glaciological studies in West Antarctica, 1960–1962," *Antarctic Snow and Ice Studies*. (Antarctic Research Series, vol. 2, series 37). Washington, D. C.: Nat. Acad. Sci., 1964.
[11] A. D. Watt and E. L. Maxwell, "Measured electrical properties of snow and glacial ice," *J. Res. Nat. Bur. Stand.*, vol. 64D, no. 4, p. 357, 1960.
[12] I. C. Peden, G. E. Webber, and A. S. Chandler, "Complex permittivity of the Antarctic ice sheet in the VLF band," *Radio Sci.*, vol. 7, no. 6, p. 645, 1972.
[13] G. E. Webber and I. C. Peden, "VLF ground-based measurements in Antarctica: their relationship to stratification in the subsurface terrain," *Radio Sci.*, vol. 5, no. 4, p. 655, 1970.
[14] E. W. Seeley and P. H. Wiborg, Jr., "Horizontal VLF transmitting antennas near the earth, Naval Ordnance Lab., Corona, Calif., NOLC Rep. 721, 1967.
[15] A. D. Watt, *VLF Radio Engineering*. New York: Pergamon, 1967.
[16] R. R. Scarabucci, "Interpretation of VLF signals observed on the OGO-4 satellite," Radioscience Lab., Stanford Univ., Stanford, Calif., Tech. Rep. 3418-2, 1969.

Waveguide-Fed Spherical Dielectric Antennas

A. G. MARTIN AND A. J. A. OXTOBY

***Abstract*—The results of an experimental investigation into the radiation properties of circular waveguide excited dielectric sphere antennas are reported. The input waveguide had a plain end without a flange or ground plane. The input voltage standing-wave ratio varied from about 1.1 to 2.5 for the sphere sizes used but can usually be reduced to about 1.25 over the 8–12 GHz band by separating the sphere from the waveguide. Separation increases the on-axis gain by 1–3 dB and produces nearly equal beamwidths in both *E*- and *H*-planes. Phase front measurements located a fixed phase center near the end of the waveguide.**

Manuscript received July 16, 1973; revised September 19, 1973.
The authors are with the Department of Electronic Engineering, University of Hull, Hull, England.

Introduction

Recently Chatterjee and Croswell [1] reported that waveguide-fed dielectric spheres could offer gains 3 dB or more in excess of that of an optimum horn [2] with the same cross-sectional area. Other workers have given results for spheres backed by metal hemispheres [3] and have shown further improvements by matching the sphere/air boundary [4].

The work described here concerns experiments between 8 and 12 GHz on paraffin wax spheres ($\epsilon_r = 2.06$) placed in front of, but displaced from, the open end of a 2.5 cm internal diameter circular waveguide carrying the TE_{11} mode (Fig. 1). No flanges or backing plates were used. The spheres were supported by a polystyrene foam surround.

A range of sphere sizes was used and specimen results for three diameters, 4.15 cm, 6.60 cm, and 8.85 cm, are discussed.

Observations

As the wax sphere is offset by d cm from the waveguide end, the input voltage standing-wave ratio (VSWR) varies periodically as shown in Fig. 2(a) for the 8.85 cm sphere. Such behaviour is similar to the input VSWR variation of a horn as the flare length is increased. Unfortunately the position of minimum VSWR shown in Fig. 2(a) is not independent of frequency. However, an optimum value of d (shown dotted in Fig. 2(a)) can be chosen where the input VSWR is low and its variation over the frequency range is minimized. The optimum value of d was found to lie between 1.0 and 1.2 cm for the three sphere sizes tested.

Input VSWR measurements for the three spheres placed at the waveguide mouth are shown in Fig. 2(b). Although the VSWR is less than 3 in these measurements, appreciable variation over the frequency range can be seen. Choosing the optimum value of d for each sphere improves the input match as shown in Fig. 2(c). For the larger spheres, input VSWR less than 1.3 was achieved over most of the 8–12 GHz range.

On-axis gain graphs for the three sphere sizes are shown in Fig. 3. With the spheres at the waveguide mouth, a gain of 2–3 dB for the two smaller spheres and about 1 dB for the largest sphere, over the optimum horn gain [2], were observed. Curves marked M are for d at the value, for each sphere, which was chosen to be optimum from the VSWR measurements. This optimum d produces an additional gain of about 2 dB. Even greater gain, compared with that of an optimum horn, has been reported elsewhere [1], [3], [4] with spheres of higher dielectric constant.

Phase fronts were measured by injecting the received signal, transmitted by the test antenna, into one end of a slotted line and injecting a reference signal, from the oscillator, into the other end. Isolators were included to avoid unwanted reflections. Rotating the test antenna shifts the minimum in the slotted line. The phase center was located by fitting a circle to the minimum positions. E- and H-plane measurements showed the phase center position to be located, to an estimated accuracy of 5 mm at worst, at the plane of the waveguide mouth and independent of frequency. Displacing the spheres had no apparent effect on the phase center position.

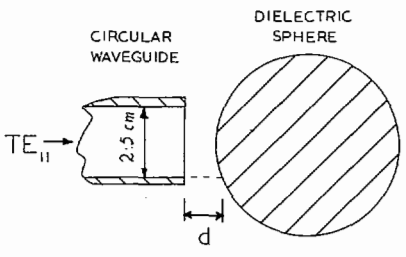

Fig. 1. Antenna arrangement.